PERFORMANCE EVALUATION OF U-Mo/Al DISPERSION FUEL BY CONSIDERING A FUEL-MATRIX INTERACTION

HO JIN RYU[*1], YEON SOO KIM[2], JONG MAN PARK[1], HEE TAEK CHAE[1] and CHANG KYU KIM[1]
[1]Recycled Fuel Development Division, Korea Atomic Energy Research Institute,
150 Deokjin-dong, Yuseong-gu, Daejeon 305-353, Republic of Korea
[2]Nuclear Engineering Division, Argonne National Laboratory,
9700 S. Cass Ave, Argonne, IL 60439, USA
[*]Corresponding author. E-mail : hjryu@kaeri.re.kr

Received July 3, 2007
Accepted for Publication March 28, 2008

Because the interaction layers that form between U-Mo particles and the Al matrix degrade the thermal properties of U-Mo/Al dispersion fuel, an investigation was undertaken of the undesirable feedback effect between an interaction layer growth and a centerline temperature increase for dispersion fuel. The radial temperature distribution due to interaction layer growth during irradiation was calculated iteratively in relation to changes in the volume fractions, the thermal conductivities of the constituents, and the oxide thickness with the burnup. The interaction layer growth, which is estimated on the basis of the temperature calculations, showed a reasonable agreement with the post-irradiation examination results of the U-Mo/Al dispersion fuel rods irradiated at the HANARO reactor. The U-Mo particle size was found to be a dominant factor that determined the fuel temperature during irradiation. Dispersion fuel with larger U-Mo particles revealed lower levels of both the interaction layer formation and the fuel temperature increase. The results confirm that the use of large U-Mo particles appears to be an effective way of mitigating the thermal degradation of U-Mo/Al dispersion fuel.

KEYWORDS : Fuel Performance, Dispersion Fuel, U-Mo, Research Reactor, Interdiffusion

1. INTRODUCTION

Dispersion fuel such as U-Mo/Al is being developed as high uranium density metallic fuel for advanced research reactors to replace the highly enriched uranium (HEU) fuel with low-enriched uranium (LEU) fuel, because U-Mo alloys have a high uranium density and an excellent irradiation stability when compared with existing fuels such as U_3Si and U_3Si_2 [1-3]. The typical microstructure of U-Mo/Al dispersion fuel consists of U-Mo alloy particles distributed in an Al matrix. The irradiation behavior of U-Mo/Al dispersion fuel has been investigated to estimate its fuel performance during irradiation [4,5]. When U-Mo/Al dispersion fuel is irradiated in reactors, radiation-induced microstructural changes occur and they influence the fuel performance of the U-Mo/Al dispersion fuel. The main change comes from the interdiffusion between the U-Mo and Al forming interaction layers [6-10]. While $(U,Mo)Al_x$, which is a mixture of intermetallic compounds of $(U,Mo)Al_2$, $(U,Mo)Al_3$, and $(U,Mo)Al_4$, has been obtained from out-of-pile annealing tests, the interaction layer becomes amorphous during irradiation at a low temperature [8-10]. Unfortunately, because the interaction layer has a lower thermal conductivity when compared to the dispersion fuel meat, the thermal conductivity of the fuel meat decreases during irradiation and then the centerline temperature of the dispersion fuel rod increases. The growth of the interaction layer is interactively affected by the temperature of the fuel because it is associated with a diffusion reaction, which is a thermally activated process. It is difficult to estimate the temperature profile of a fuel rod during an irradiation test due to the interdependency of the fuel temperature and the thermal conductivity, both of which are changed by the interaction layer growth, although the temperature distribution at the beginning of life can be calculated on the basis of the initial condition of irradiation and the as-fabricated microstructure of a fuel rod.

In this study, the temperature histories of U-Mo/Al dispersion fuel during irradiation tests were estimated by considering the effect of an interaction layer growth on the thermal conductivity of the fuel meat. In addition, the fuel performance behavior of the U-Mo/Al dispersion fuel was estimated by a combination of empirical models obtained from the post-irradiation examination (PIE) data of the U-Mo/Al dispersion fuel.

2. ANALYSIS PROCEDURES

The fuel temperature of a U-Mo/Al dispersion fuel rod was calculated by solving a cylindrical heat transfer equation with the aid of the thermal conductivities of the dispersion fuel meat, Al clad, and oxide film. The thermal conductivity of the commercially pure aluminum (Al1060) matrix used in this study is 220 (W/mK). Because no data for an irradiated sample of (U,Mo)Al_x is available, we used the best available thermal conductivity for the interaction layer. Recent PIE results showed that x is around 3 to 4 for the HANARO irradiation conditions and Mo is considered to have a minor effect on the thermal conductivity because its amount in the interaction layer is small when compared to the other constituents. The thermal conductivity of the U-Mo alloys is expressed as a function of the temperature as follows [11]:

$$k_{UMo} = 0.034T - 0.56 \ \text{(W/mK)}, \tag{1}$$

where T is the absolute temperature (K).

The effect of irradiation on the thermal conductivity of the Al matrix was not included in this study. Because the void swelling rate of aluminum is near zero at around 150°C due to a self-annealing or a recombination of the radiation defects [11], only the fission gas bubble in the U-Mo particle was considered as a major degradation mechanism of the thermal conductivity.

The thermal conductivity of the dispersion fuel meat was calculated on the basis of a modified Hashin and Shtrikman relation, the so-called auto-coherent law, which was developed by CEA as follows [12,13]:

$$k = \frac{-k_c + 3V_c k_c + 2k_m - 3V_c k_m + \sqrt{8k_c k_m + (k_c - 3V_c k_c - 2k_m + 3V_c k_m)^2}}{4}, \tag{2}$$

where k_c and k_m are the thermal conductivities of the U-Mo/interaction layer composite particle and the Al matrix, respectively, and V_c is the volume fraction of the composite particle. The effective thermal conductivity of a U-Mo/interaction layer composite particle, k_c, was obtained as follows [13,14]:

$$\frac{1}{k_c} = \frac{1}{k_{UMo}}\left(1 - \frac{Y}{R}\right) + \frac{1}{k_{IL}}\left(\frac{Y}{R}\right), \tag{3}$$

where k_{UMo} and k_{IL} are the thermal conductivities of the U-Mo and the interaction layer, respectively; Y is the thickness of the interaction layer; and R is the radius of the composite particle. The thermal conductivity of the interaction layer was assumed to be 10 (W/mK) on the basis of the thermal conductivities of UAl_3 and UAl_4 as measured by Nazare *et al*. [15].

The porosity effect was incorporated into the thermal conductivity of the fuel particle by using an exponential decay factor as follows [16]:

$$k_P = k_{100} \cdot \exp(-2.14 \cdot P), \tag{4}$$

where k_p is the thermal conductivity of a material with a porosity of P, k_{100} is the thermal conductivity of a fully dense material (k_{UMo} in Eq.(1)), and P is a porosity fraction from 0 to 1. This correlation is valid for porosities below 0.3. When atomized powder is used, the dispersion fuel reveals nearly a full density (P<0.01) after a hot extrusion; hence, the porosity is mainly due to the formation of the fission gas bubbles in the fuel particles. The porosity in the U-Mo particles was calculated from a fuel swelling correlation because 25 percent of the total fuel swelling is known to be due to fission gas bubbles according to an empirical correlation obtained from the RERTR irradiation tests [14].

An empirical correlation for an interaction layer growth was developed from the results of the RERTR irradiation tests as follows [14]:

$$Y^2 = A \cdot \dot{f}^{1/2} \cdot \Delta t \cdot \exp\left(\frac{-Q}{RT}\right) \tag{5}$$

where Y is the interaction layer thickness (cm), $\dot{f}$ is the effective fission rate density (fissions/cm^3-s), Δt is the time interval (s), R is the ideal gas constant, and T is the absolute temperature (K). The pre-exponential constant, A ($cm^{7/2}$/fissions$^{1/2}$-$s^{1/2}$), and the activation energy, Q (kJ/mol), can be obtained by comparing the interaction layer thicknesses with the calculation results and the PIE microstructures.

The swelling of a U-Mo particle due to solid fission products and fission gas bubbles was estimated according to an empirical correlation obtained from the RERTR irradiation tests. Kim *et al*. proposed a two-step swelling correlation because the swelling rate increases after a critical burnup at which a recrystallization of U-Mo occurs as follows [17]:

$$\frac{\Delta V}{V_0} = 6 \times 10^{-23} \cdot f, \quad \text{for } f \le 3 \times 10^{21} \text{ fissions/cm}^3 \tag{6}$$

$$\frac{\Delta V}{V_0} = 12.3\times10^{-23}\cdot f - 0.189, \quad \text{for } f \geq 3\times10^{21} \text{ fissions/cm}^3, \tag{7}$$

where f is the fission density of the U-Mo (fissions/cm^3). The effect of the Mo content on the correlation was not considered in this study because 7 wt% to 10 wt% Mo showed a similar swelling behavior in the recent RERTR irradiation experiments [17].

There is another swelling linked to an interaction layer formation because the density of an interaction layer is not the same as the average of the reaction constituents U-Mo and Al. The swelling is expressed as follows:

$$V_{IL}/V_{UMo/Al} = \frac{\dfrac{M_{UMo}+x\cdot M_{Al}}{\rho_{IL}}}{\dfrac{M_{UMo}}{\rho_{UMo}}+x\cdot\dfrac{M_{Al}}{\rho_{Al}}} \tag{8}$$

where V_{IL} is the volume of the interaction layer; $V_{UMo/Al}$ is the volume of the dispersion fuel; M_{UMo} and M_{Al} are the molar weights of the U-Mo alloy and Al, respectively; and ρ_{IL}, ρ_{UMo}, ρ_{Al} are the densities of the interaction layer, U-Mo, and Al, respectively. Hofman and Meyer proposed a correlation for the density of (U,Mo)Al_x, for the range $2 < x < 4.5$ as follows [11]:

$$\rho_{(U,Mo)Alx} = 9.38 - 0.98x \qquad (\text{g/cm}^3). \tag{9}$$

However, an aluminum-rich interaction layer with a high x (x=4.5–7) was observed in the plate-type irradiation test, and data does not exist in the literature for the densities of the interaction layers that form during irradiation. The density of the aluminum-rich interaction layer was extrapolated using Eq. (9) and the density of aluminum (2.7 g/cm^3).

The thickness of the oxide film on the outside of the clad was obtained from the Griess model [18,19], which has the following basic form:

$$x = \left(x_0^{\,1.28535} + 1.28535\,k\,t\right)^{0.778}, \tag{10}$$

where x is the oxide film thickness at time t, $x_0$is the initial oxide film thickness, t is the time in hours, and k is the rate constant expressed by

$$k = 1.2538\times10^5 \exp\left(\frac{-5913}{T_i}\right), \tag{11}$$

Table 1. Operating Conditions of the HANARO Reactor

Items	Conditions
Coolant	H_2O
Core inlet temperature	35°C
Core outlet temperature	45°C
Core inlet pressure	0.409 MPa
Core outlet pressure	0.2 MPa
Core flow velocity	7.3 m/s

where T_i is the temperature at the oxide-water interface in K. In this study, the oxide-metal interface temperature was used for the oxidation film thickness calculation.

The fuel temperature was calculated by using the thermal conductivities of the components obtained from a calculation. The fuel rod was simulated as four concentric rings of equal thickness with thermal conductivities that differed according to the volume fraction of the interaction layer because a different volume fraction for an interaction

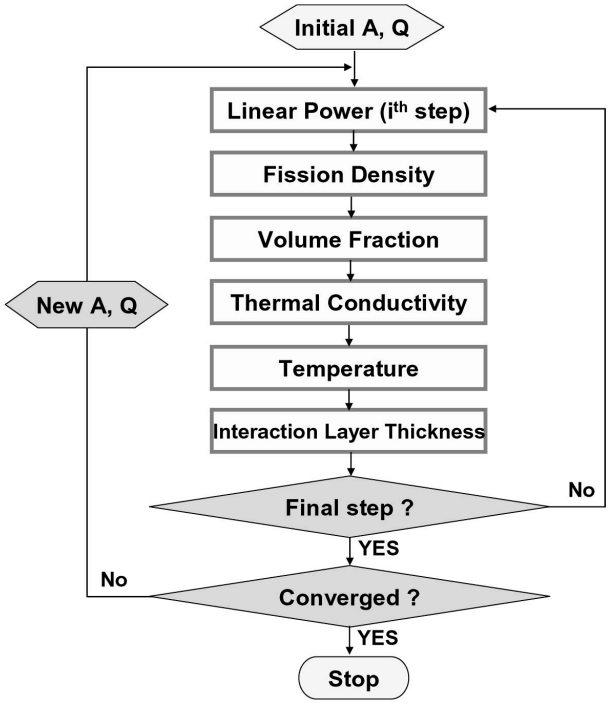

Fig. 1. Flow Chart of the Fuel Temperature Calculation Procedures used in this Study

Table 2. Particle Size Distributions of the Reference U-7Mo Powder and Two Different Particle-Sized Powder used in the KOMO-2 Irradiation Test

Size	Reference Powder	Fine Powder	Coarse Powder
38–45 μm	33.7%	11.1%	
45–53 μm	18.5%	59.2%	
53–63 μm	23.4%	29.7%	36.3%
63–75 μm	17.9%		40.0%
75–90 μm	4.3%		19.3%
90–106 μm	0.2%		4.4%
106–125 μm	1.0%		
125– μm	1.0%		

layer along the radial direction results in an axisymmetric variation of the thermal conductivities. A cylindrical heat transfer equation with the boundary conditions of the HANARO cooling system, as shown in Table 1, was used in this study.

Fig. 1 shows a flow chart for the fuel temperature calculation procedures of this study. An interaction layer thickness corresponding to each burnup was calculated by using the interaction layer growth correlation, that is, Eq. (5). After considering the swelling caused by fission gas bubbles, fission products, and interaction layers, we calculated the thermal conductivity of the dispersion fuel meat by considering the volume fraction of the interaction layer, the U-Mo fuel, and the Al matrix at each burnup. The fuel temperature was then calculated by using the thermal conductivities of each phase, and the calculation procedures subsequently moved on to the interaction thickness calculation of the next burnup step. More detailed descriptions of the calculation procedures are given in [22].

The temperature histories of the second U-Mo/Al dispersion fuel irradiation tests (KOMO-2) at HANARO were analyzed in terms of reactor operation histories, fuel fabrication specifications and PIE results [20,21]. In the KOMO-2 test, a U-7Mo/Al dispersion fuel rod with a diameter 6.35 mm and 4.0 gU/cm^3 (494L2) and a U-7Mo/Al dispersion fuel rod with a diameter of 5.49 mm and 4.5 gU/ cm^3 (494H2) were irradiated up to a 71% U-235 (14% FIMA) peak burnup in 2003. The unit of a burnup, at.% U-235, used in this study represents a percentage of the fissioned U-235 atoms to the initial U-235 atoms loaded in the U-Mo fuel. This unit can be converted to another burnup unit, FIMA, by multiplying the LEU enrichment, 19.75 wt% (19.95 at%). The bottom section of the KOMO-2 494H2 fuel rod (4.5 gU/ cm^3, 50% U-235

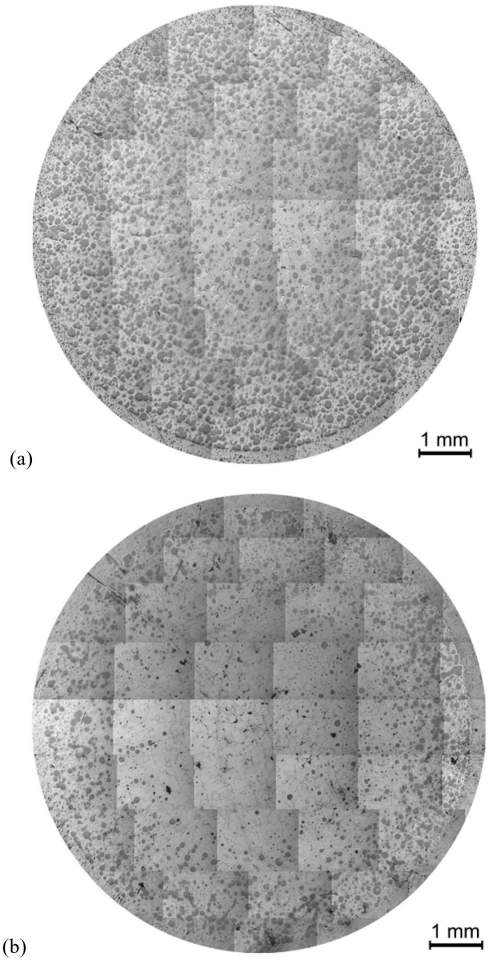

Fig. 2. End-of-Life Cross-Sectional Microstructures of the 494H2 Fuel Rod at Two Different Cross Sections: (a) the Bottom Position (50% U-235 Burnup) and (b) the Middle Position (62% U-235 Burnup)

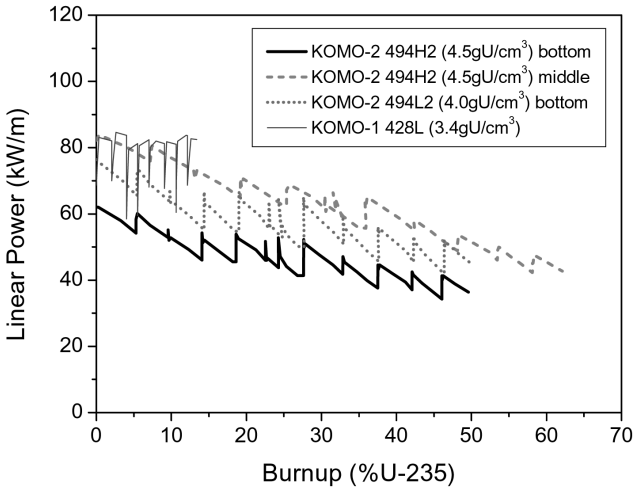

Fig. 3. Linear Power Histories of the Bottom Section and the Middle Section of the 494H2 Fuel Rod, and the Bottom Section of 494L2 in the KOMO-2 Irradiation Test, as Well as the Linear Power History of the 428L Fuel Rod in the KOMO-1 Irradiation Test

burnup) was used as a reference, and the middle section of the KOMO-2 494H2 (4.5 gU/cm^3, 62% U-235 burnup), the bottom section of the KOMO-2 494L2 (4.0 gU/ cm^3, 50% U-235 burnup), as well as the KOMO-1 428L (3.4 gU/cm^3, 13% U-235 burnup) were used to validate the interaction layer growth correlation formulated in this study. The volume fractions of U-Mo (V_{UMo}) for 3.4 gU/cm^3, 4.0 gU/cm^3, and 4.5 gU/cm^3, were estimated to be 0.21, 0.25, and 0.29, respectively.

The particle size distributions of the reference U-7Mo powder used in the KOMO-2 irradiation test are listed in Table 2. In addition, two different particle-sized U-7Mo powders were used to fabricate two more dispersion fuel rods irradiated in this study in order to investigate the effect of the U-Mo particle size on the irradiation behavior. The particle size distributions of the two different particle-sized U-7Mo powders used in the KOMO-2 irradiation test are also listed in Table 2.

A PIE was conducted at the Irradiation Material Examination Facility of KAERI in 2004. Fig. 2 shows cross-sectional images of the 494H2 fuel rod at the bottom, where the end-of-life burnup is estimated to be 50% U-235, and the 494H2 fuel rod at the middle, where the end-of-life burnup is estimated to be 62% U-235. The bottom cut was selected as a reference cross section to obtain the constants for an interaction layer growth correlation because a large variation of the interaction layer thickness from the center to the periphery provided better accuracy for a fitting.

Fig. 3 plots the linear power histories for the bottom section of the 494H2 fuel rod, the middle section of the

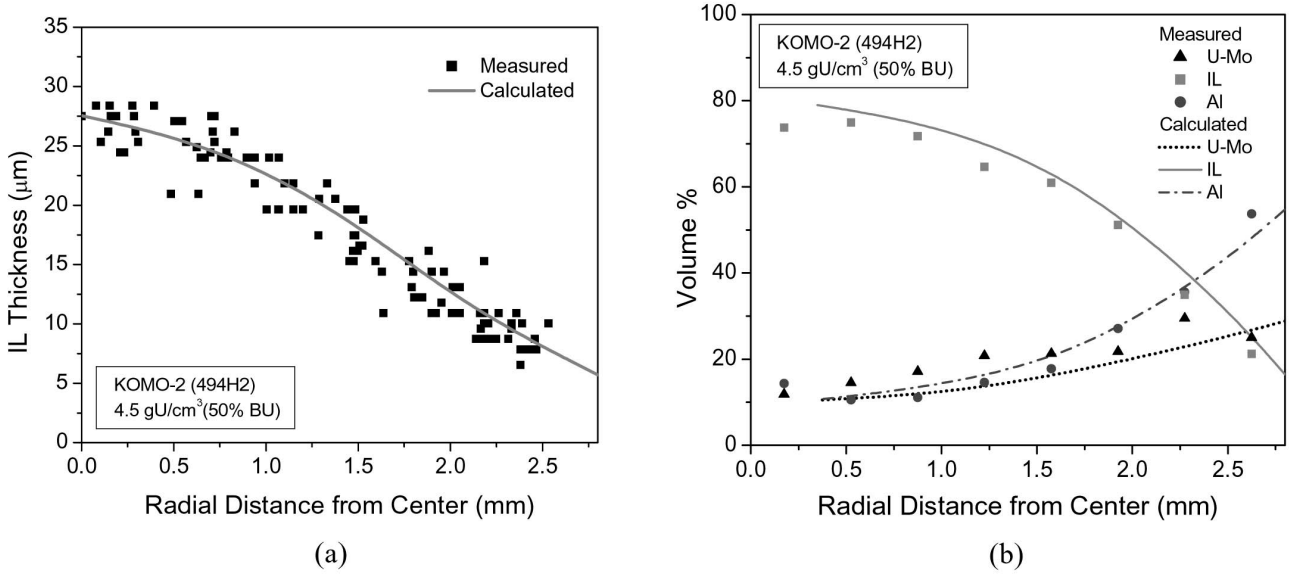

Fig. 4. Comparison of the Microstructural Measurement Obtained from the Post-Irradiation Examination and the Calculation Results: (a) for the Radial Distribution of the Interaction Layer Thicknesses and (b) for the Volume Fractions of the Constituents in the Bottom Section of 494H2 Fuel Rod

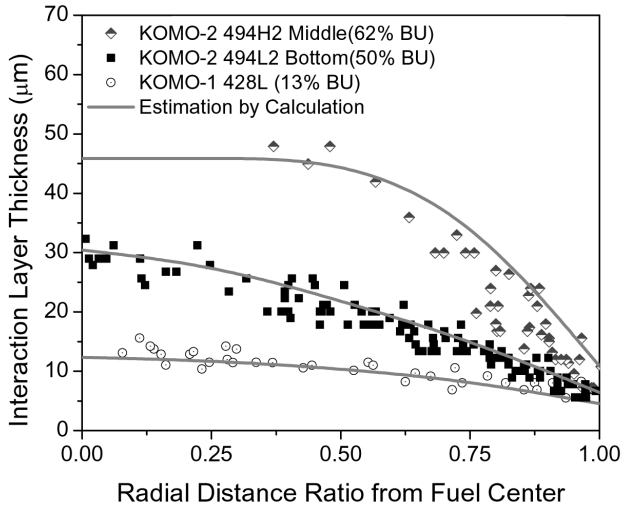

Fig. 5. Comparison of the Measured Interaction Layer Thicknesses and the Calculated Interaction Layer Thicknesses of KOMO-2 494L2 (50% U-235 burnup), KOMO-2 494H2 (62% U-235 Burnup), and KOMO-1 428L (13% U-235 Burnup)

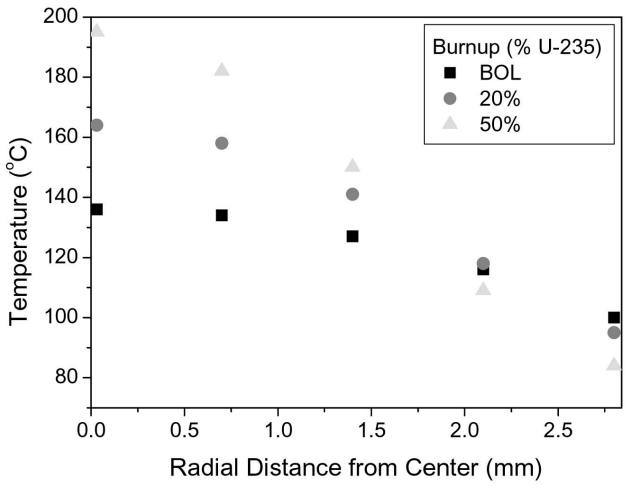

Fig. 6. The Variation of the Radial Temperature Profile with a Burnup (494H2 Bottom Section)

494H2 fuel rod, and the bottom section of the 494L2 fuel rod, as well as the KOMO-1 428L fuel rod with a burnup.

3. RESULTS AND DISCUSSION

Kim *et al*. showed that the activation energy in Eq. (5) was a function of the irradiation temperature [22]. They proposed two different activation energies for low temperature (<393 K) and high temperature (>393 K) irradiation conditions. While an irradiation at a low temperature resulted in a higher activation energy, a lower activation energy was obtained for the high temperature irradiation tests. The experimental results, such as the radial distribution of the interaction layer thickness obtained from the PIE for the KOMO-2 fuel, were compared with the calculation results as shown in Fig. 4(a). The best fit for the reference rod-cut was

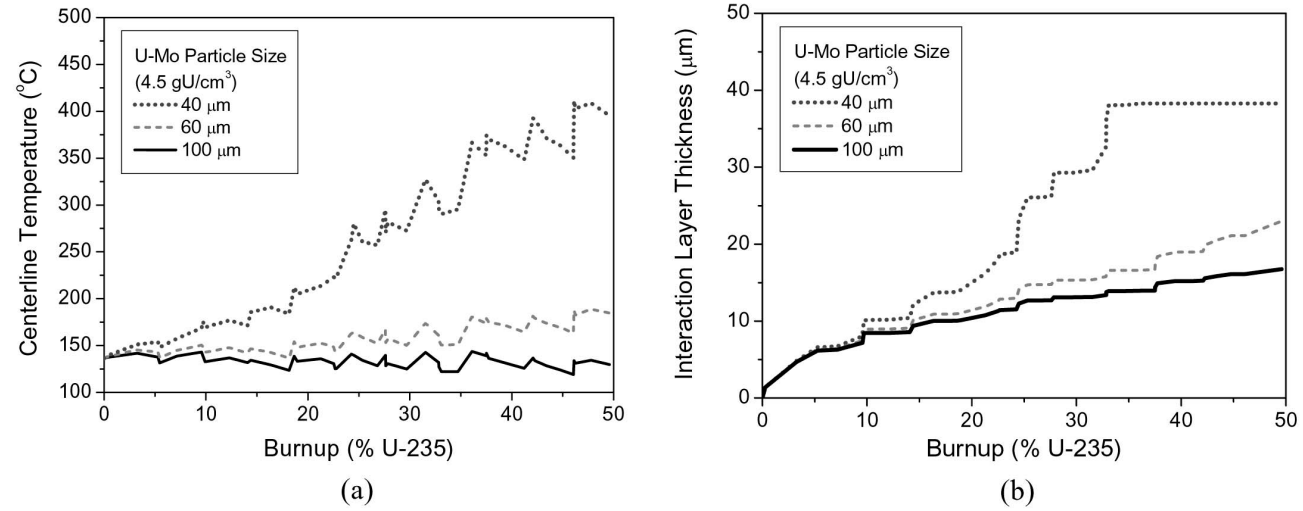

Fig. 7. (a) Variation of the Centerline Temperature and (b) Variation of the Interaction Layer Thickness in the Center Zone of the 4.5 gU/cm^3 Dispersion Fuel with a Varying U-Mo Particle Size (Linear Power of 494H2 Bottom)

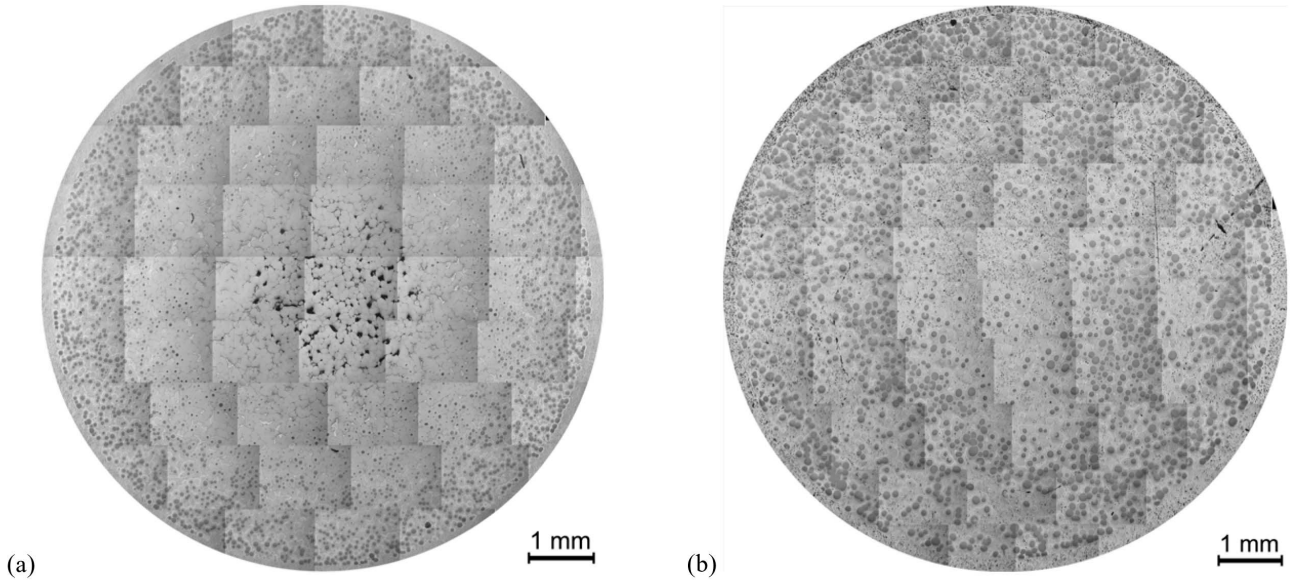

Fig. 8. End-of-Life Microstructures of the Dispersion Fuel with (a) Fine U-Mo Powder (38–63 μm) and (b) Coarse U-Mo Powder (53–106 μm) in the KOMO-2 Irradiation Test

obtained when the following interaction layer growth correlations were used:

$$Y^2 = 2.1\times10^{-11}\cdot \dot{f}^{1/2}\cdot\Delta t\cdot\exp\left(\frac{-71.4\,kJ/mol}{RT}\right) \quad \text{when T<393 K} \tag{12}$$

$$Y^2 = 1.1\times10^{-15}\cdot \dot{f}^{1/2}\cdot\Delta t\cdot\exp\left(\frac{-37.8\,kJ/mol}{RT}\right) \quad \text{when T>393 K} \tag{13}$$

where Y is the interaction layer thickness (cm), $\dot{f}$ is the effective fission rate density (fissions/cm^3-s), Δt is the

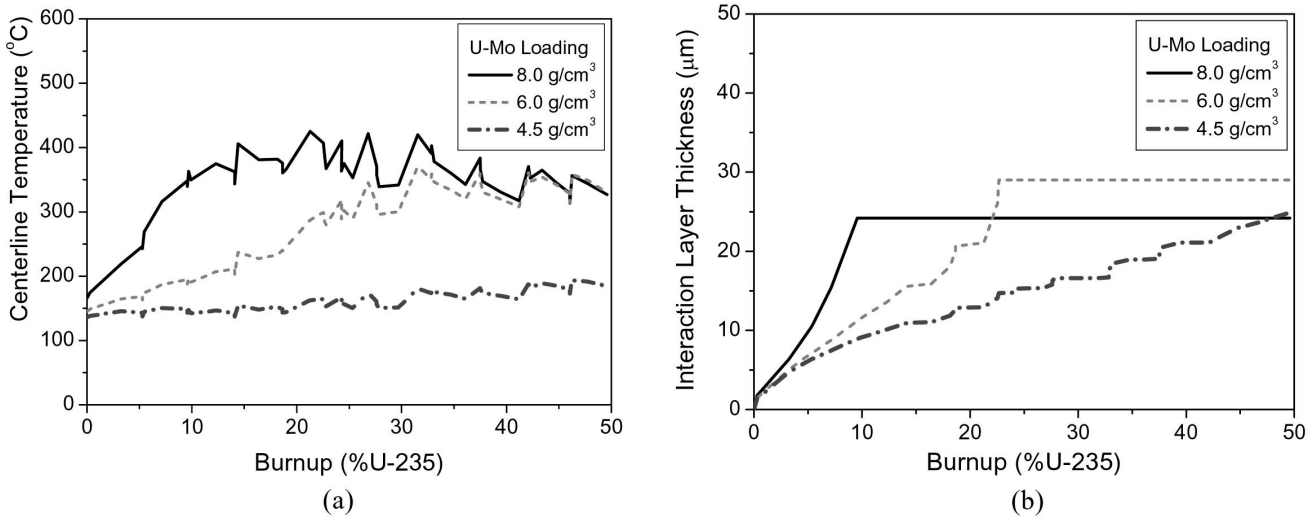

Fig. 9. Effects of a Uranium Loading (a) on a Variation of the Fuel Temperature and (b) on a Variation of the Interaction Layer Thickness in the Center Zone with an Increasing Burnup (Linear Power of 494H2 Bottom)

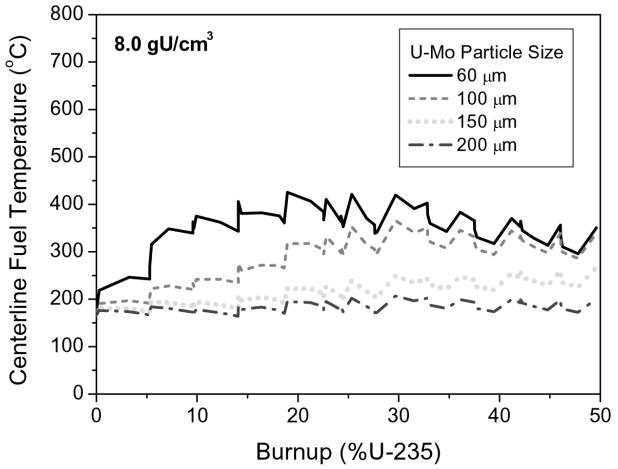

Fig. 10. Calculated Fuel Temperature of a 8 gU/cm^3 U-Mo/Al Dispersion Fuel with a Varying Fuel Particle Size

time interval (s), *R* is the ideal gas constant, and *T* is the absolute temperature (K). As shown in Fig. 4(b), the end-of-life volume fractions for the U-Mo, the Al matrix, and the interaction layer, which were measured by means of image analysis of the PIE micrographs, show a reasonable agreement when compared to the calculated volume fractions.

Fig. 5 presents the comparison results of the measured interaction layer thicknesses and the calculated thicknesses for the bottom section of KOMO-2 494L2 (50% U-235 burnup, 4.0 gU/cm^3), the middle section of KOMO-2 494H2 (62% U-235 burnup, 4.5 gU/cm^3), and the KOMO-1 428L (13% U-235 burnup, 3.4 gU/cm^3). The interaction layer thickness distribution calculated for the fuel rods with various linear power histories revealed a good estimation with the same correlation developed in this study.

Fig. 6 shows the radial temperature profiles with a burnup for the bottom section of the 494H2 rod. Because the thermal conductivity of the fuel meat decreases with the burnup due to the growth of an interaction layer, the temperature gradient becomes steeper at a higher burnup.

Fig. 7 shows the effect of the U-Mo particle size on the centerline temperature and on the interaction layer thickness when the average diameter of the U-Mo fuel particles in the 4.5 gU/cc dispersion fuel is varied from 40 μm to 100 μm. The centerline temperatures were decreased by an increase in the average diameter of the fuel particles because the specific interfacial area necessary for the interaction decreases; thus, the volume fraction of this less-conducting interaction layer increases slowly. As shown in Fig. 7(b), the interaction layer thicknesses of the center zone were also decreased by an increase in the average diameter of the fuel particles due to the lower fuel temperature in a larger particle dispersion fuel.

The effect of the U-Mo particle size was experimentally confirmed by the KOMO-2 irradiation test, which is presented in Fig. 8. When the end-of-life microstructures of the U-Mo/Al dispersion fuel with a fine U-Mo powder (38–63 μm) and a coarse U-Mo powder (53–106 μm) were compared, the dispersion fuel with the large particles exhibited a smaller volume fraction of the interaction layer. The completely reacted zone was expanded to three quarters of the radius for the dispersion fuel with the small particles, whereas only the area from the center to a quarter of the radius was converted in the dispersion fuel with the large particles.

The effect of the U-Mo loading density on the centerline temperature is shown in Fig. 9(a) when the fuel loading density is varied from 4.5 gU/cm^3 (V_{UMo}=0.29) to 8.0 gU/cm^3 (V_{UMo}=0.51). The centerline temperatures were increased by an increase in the U-Mo loading density because the larger volume fraction of the U-Mo results in lower thermal conductivity of the dispersion fuel meat. The maximum centerline temperature increased as the uranium loading density increased. When the fuel loading density is 8.0 gU/cm^3, the centerline temperature is saturated after a U-235 burnup of about 15% because the interaction layer growth is limited when the Al matrix is exhausted. As shown in Fig. 3, when the degradation of the thermal conductivity by the interaction layer formation is not progressing, the centerline temperature follows the decreasing linear power with a burnup. In addition, as shown in Fig. 9(b), the interaction layer thicknesses of the center zone were increased more rapidly in a higher uranium loading density fuel due to the higher fuel temperature. The growth of the interaction layer in a higher uranium loading density fuel was saturated earlier because of the depletion of the Al matrix.

Although a uranium density higher than 8 gU/cm^3 is needed to replace the HEU fuel with LEU fuel, the fuel temperature was estimated to rise above 300°C after the initial burnup when the uranium loading density was higher than 6 gU/cm^3. Coarse U-Mo particles up to 760 μm in diameter were fabricated by a centrifugal atomization process to overcome the limitation of a uranium loading density in U-Mo/Al dispersion fuel [23]. The centerline temperature of U-Mo/Al dispersion fuel with 8 gU/cm^3 was calculated by varying the average fuel particle size from 60 μm to 200 μm as plotted in Fig. 10. When the average fuel particle size range varied from 60 μm to 150 μm, undesirable temperature increases were predicted due to an active interaction layer growth, whereas a stable fuel temperature history was predicted when the average fuel particle size was larger than 200 μm. Dispersion of coarse U-Mo fuel particles larger than 200 μm is expected to be a remedy for interaction-related problems in a rod-type dispersion fuel with a high uranium loading density.

Although more factors such as the fins attached to a fuel rod and a radial flux depression should be included in a detailed estimation of the irradiation behavior of U-Mo dispersion fuel, the effects of an interaction layer and fuel particle size on the fuel temperature history appeared to be dominant factors according to a calculation that incorporates a burnup-wise microstructural evolution during irradiation.

4. CONCLUSION

The fuel temperature history of rod-type U-Mo/Al dispersion fuel was calculated by considering an interaction layer growth during irradiation. The fuel temperature of the rod-type dispersion fuel showed a strong feedback behavior due to a lower thermal conductivity of the interaction layer. The estimated fuel temperature increased as the U-Mo particle size decreased or the uranium loading density increased. The dispersion of a larger U-Mo particle was found to be effective for mitigating the thermal degradation that is associated with an interaction layer growth.

ACKNOWLEDGMENTS

This study was supported by the National Nuclear R&D Program of the Korean Ministry of Education, Science and Technology (MEST).

REFERENCES

[1] J.L. Snelgrove, G.L. Hofman, M.K. Meyer, C. L. Trybus and T. C. Wiencek, "Development of Very-high-density Low-enriched-uranium Fuels," *Nucl. Eng. Des*., **178**, 119 (1997).

[2] G.L. Hofman and Y.S.Kim, "A Classification of Uniquely Different Types of Nuclear Fission Gas Behavior," *Nucl. Eng. Technol*., **37**, 299 (2005).

[3] C.K.Kim, J.M.Park, and H.J.Ryu, "Use of a Centrifugal Atomization Process in the Development of Research Reactor Fuel," *Nucl. Eng. Technol*., **39**, 617 (2007).

[4] M.K. Meyer, G.L. Hofman, S.L. Hayes, C.R. Clark, T.C. Wiencek, J. L. Snelgrove, R. V. Strain and K. -H. Kim, "Low-temperature Irradiation Behavior of Uranium–molybdenum Alloy Dispersion Fuel," *J. Nucl. Mater*., **304**, 221 (2002).

[5] A. Leenaers, S. Van den Berghe, E. Koonen, C. Jarousse, F. Huet, M. Trotabas, M. Boyard, S. Guillot, L. Sannen and M. Verwerft, "Post-irradiation Examination of Uranium–7 wt% Molybdenum Atomized Dispersion Fuel," *J. Nucl. Mater*., **335**, 39 (2004).

[6] D.B. Lee, K.H. Kim and C.K. Kim, "Thermal Compatibility Studies of Unirradiated U-Mo Alloys Dispersed in Aluminum," *J. Nucl. Mater*., **250**, 79 (1997).

[7] K.H. Kim, D.B. Lee, C.K. Kim, G.L. Hofman and K.W. Paik , "Thermal Compatibility of Centrifugally Atomized U–Mo Powders with Aluminum in a Dispersion Fuel," *Nucl. Eng. Des*., **178**, 111 (1997).

[8] H.J. Ryu, Y.S. Han, J.M. Park, S.D. Park and C.K. Kim, "Reaction Layer Growth and Reaction Heat of U–Mo/Al Dispersion Fuels Using Centrifugally Atomized Powders," *J. Nucl. Mater*., **321**, 210 (2003).

[9] H.J. Ryu, Y.S. Kim, G.L. Hofman, D.D. Keiser, "Characterization of the Interaction Products in U-Mo/Al Dispersion Fuel from In-pile and Out-of-pile Tests," *Proc. RERTR-2006 Inter. Mtg*., Cape Town, South Africa, Oct. 29-Nov.2, 2006.

[10] S. Van den Berghe, W. Van Renterghem and A. Leenaers, "Transmission Electron Microscopy Investigation of Irradiated U-7wt%Mo Dispersion Fuel," *J. Nucl. Mater*., **375**, 340 (2008).

[11] G.L. Hofman and M.K. Meyer, "Properties of U–Mo Alloy Dispersion Fuel," *IAEA Technical Meeting on the Development of High Density Uranium–Molybdenum Dispersion Fuel*, Vienna, Austria, Jun. 23-25, 2003.

[12] Z. Hashin and S. Shtrikman, "A Variational Approach to the Theory of the Effective Magnetic Permeability of Multiphase Materials," *J. Appl. Phys*., **33**, 3125 (1962).

[13] V. Marelle, F. Huet, P. Lemoine, "Thermo-Mechanical Modelling of U-Mo Fuels with MAIA," *8th Inter. Mtg. on RRFM*, Munich, Germany, Mar. 21-24, 2004.

[14] S.L. Hayes, M.K. Meyer, G.L Hofman and J.L. Snelgrove, "U-Mo/Al Dispersion Fuel Modeling," *Technical Meeting on the Development of High Density U-Mo Dispersion Fuels*, Vienna, Austria, June 23-25, 2003.

[15] S. Nazaré, G. Ondracek and F. Thümmler, "Investigations on UAlx-Al Dispersion Fuels for High-flux Reactors," *J. Nucl. Mater*., **56**, 251, (1975).

[16] M.E. Cunningham and K.L. Peddicord, "Heat Conduction in Spheres Packed in an Infinite Regular Cubical Array," Inter. *J. Heat Mass Transfer*, **24**, 1081 (1981).

[17] Y.S. Kim, G.L. Hofman, P.G. Medvedev, G.V. Shevilykov, A.B. Robinson and H.J. Ryu, "Post Irradiation Analysis and Performance Modeling of Dispersion and Monolithic U-Mo Fuels," *Proc. RERTR-2007 Inter. Mtg*., Prague, Czech, Sep. 23-27, 2007.

[18] J.C. Griess, H.C. Savage and J.L. English, "Effect of Heat Flux on the Corrosion of Aluminum by Water. Part IV. Tests Relative to the Advanced Test Reactor and Correlation with Previous Results," ORNL-3541, Oak Ridge National Laboratory (1964).

[19] Y.S. Kim, G.L. Hofman, A.B. Robinson, J.L. Snelgrove, N.A. Hanan, "Oxidation of Aluminum Alloy Cladding for Research and Test Reactor Fuel," *J. Nucl. Mater*., **378**, 220 (2008).

[20] C.K. Kim, Y.S. Lee, D.B. Lee, S.J. Oh, K.H. Kim, H.T. Chae, J.M. Park, D.S. Sohn, "Status of the Back-end Optional Advanced Research Reactor Fuel Development in Korea," *Proc. RERTR-2003 Inter. Mtg*., Chicago, USA. Oct. 5-10, 2003.

[21] J.M. Park, H.J. Ryu, Y.S. Lee, D.B. Lee, S.J. Oh, B.O. Ryu, Y.H. Jung, D.S. Sohn, and C.K. Kim, "An Investigation on the Irradiation Behavior of Atomized U-Mo/Al Dispersion Rod Fuels," *Proc. RERTR-2004 Inter. Mtg*., Vienna, Austria, Nov. 7-12, 2004.

[22] Y.S. Kim, G.L. Hofman, H.J. Ryu and S.L. Hayes, "Irradiation-enhanced Interdiffusion in the Diffusion Zone of U-Mo Dispersion Fuel in Al," *J. Phase Equil. Diff*., **27**, 614 (2006).

[23] C.K. Kim, K.H. Kim, J.M. Park, H.J. Ryu, Y.S. Lee, D.B. Lee, S.J. Oh, H.T. Chae, C.G. Seo, C.S. Lee, "Progress of

the KOMO-3 Irradiation Test for Various U-Mo Dispersion and Monolithic Fuels to Overcome the Interaction Problem in U-Mo/Al Dispersion Fuel," *Proc. RERTR-2005 Inter. Mtg.*, Boston, USA, Nov. 6-10, 2005.